PERGAMON

Journal of Structural Geology 25 (2003) 307–315

JOURNAL OF STRUCTURAL GEOLOGY

www.elsevier.com/locate/jsg

Strain localisation and population changes during fault system growth within the Inner Moray Firth, Northern North Sea

J.J. Walsh[a,*], C. Childs[a], J. Imber[a], T. Manzocchi[a], J. Watterson[b], P.A.R. Nell[c]

[a]*Fault Analysis Group, Department of Geology, University College Dublin, Belfield, Dublin 4, Ireland*
[b]*Fault Analysis Group, Liverpool University Marine Laboratory, Port Erin, Isle of Man IM9 6JA, UK*
[c]*Badley Earth Sciences Ltd, North Beck Lane, Hundleby, Spilsby, Lincolnshire PE23 5NB, UK*

Received 1 September 2000; accepted 1 February 2002

Abstract

The evolution of fault populations is established for an area within the Late Jurassic Inner Moray Firth sub-basin of the North Sea. Sedimentation rates outstripped fault displacement rates resulting in the blanketing of fault scarps and the preservation of fault displacement histories. Displacement backstripping is used to establish the growth history of the fault system.

Fault system evolution is characterised by early generation of the main fault pattern and progressive localisation of strain onto larger faults. This localisation is accompanied by the death of smaller faults and an associated change in the active fault population from power-law to scale-bound. Fault length populations evolve from a power-law frequency distribution containing all faults, to a power-law distribution with a marked non-power-law tail containing the largest faults. This change in population character is synchronous with the development of a fully-connected fault system extending across the mapped area and the accommodation of displacements almost exclusively on the largest faults. Strain localisation onto fewer and better connected faults represents the most efficient means of accommodating fault-related deformation and is considered to be a fundamental characteristic of the spatio-temporal evolution of fault systems. Progressive strain localisation requires complementary changes in the characteristics of associated earthquake populations.

Keywords: Strain localisation; Fault system growth; Fault populations

1. Introduction

The size populations of ancient tectonic fault systems are often described by power-law distributions (Fig. 1a), in which the relative numbers of large to small faults is consistent over a broad range of fault sizes (Kakimi, 1980; Childs et al., 1990; Scholz and Cowie, 1990; Walsh et al., 1991; Pickering et al., 1996). Fault size can be measured in different ways, but is ideally taken as either the maximum displacement across, or the maximum dimensions of, an individual fault surface. Similar power-law scaling is typical of earthquake sizes in currently active tectonic regimes and is referred to as the Gutenberg–Richter relation, for which size is usually measured as either the magnitude or the seismic moment of individual earthquakes, where seismic moment is related to the product of the displacement or slip and the surface area of fault rupture of the earthquake event (Scholz, 1989). The broad equivalence in scaling laws of faults and earthquakes is not surprising, given that tectonic faults often grow in size by the accumulation of earthquake events (Walsh and Watterson, 1987, 1988; Cowie and Scholz, 1992a,b). Power-law scaling properties are typical of fractal geometries and departures from this type of scaling law in fault or earthquake populations are often attributed to either spatial or temporal sampling effects. For example, it has been suggested that earthquake populations on the scale of individual faults or fault zones follow the characteristic earthquake model (Schwartz and Coppersmith, 1984; Wesnousky, 1994), in which the largest earthquake(s) scales with the size of the largest fault(s) and has a size(s) that is significantly larger than would be predicted from an extrapolation of the remaining earthquake population curve (Fig. 1b; Wesnousky et al., 1983; Wesnousky, 1994). A Gutenberg–Richter relation on a regional scale would therefore derive from the sum of the seismicity along many such faults, each of which may show a characteristic earthquake relation (Wesnousky, 1994, 1999). Similarly, fault populations derived from petroleum industry sub-surface datasets in ancient extensional basins are often dominated by the large faults that form the bounding structures to petroleum reservoirs, with the larger faults again

* Corresponding author. Tel.: +353-1-716-2606; fax: +353-1-716-2607.
E-mail address: john@fag.ucd.ie (J.J. Walsh).

0191-8141/02/$ - see front matter
PII: S0191-8141(02)00028-7

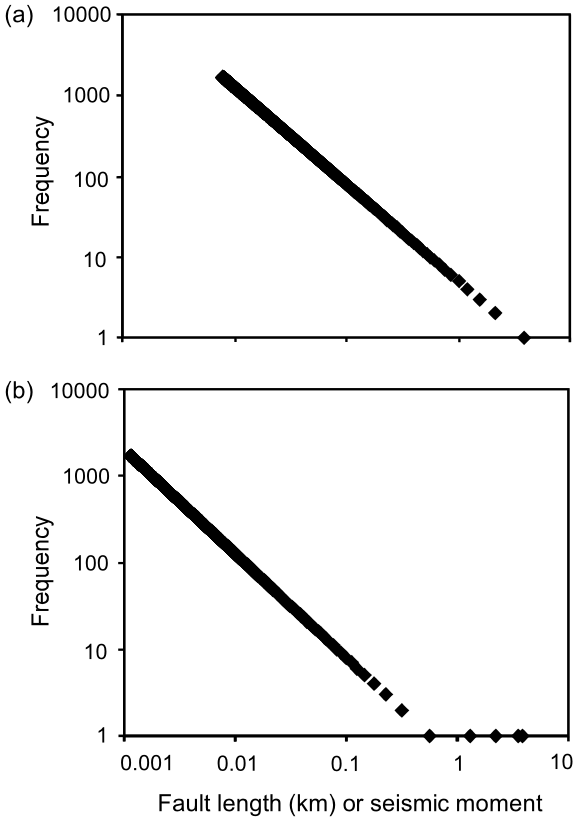

Fig. 1. Synthetic population curves for faults (fault length) or earthquakes (seismic moment) showing (a) a continuous power law over the entire range, and (b) a limited power law distribution with outsized faults or earthquakes forming a non-power law tail. Earthquake population curves of the form seen in (a) and (b) are typical of Gutenberg–Richter and characteristic earthquake behaviour, respectively.

having a size that is greater than would be expected by extrapolation of the smaller fault population curve (Walsh et al., 1994; Yielding et al., 1996). In this study, we examine the growth of a normal fault system in the North Sea and show that the fault populations change through time from power-law to non-power law. We attribute this evolution to progressive strain localisation onto larger faults and the death of smaller faults with increasing maturity of the fault system. This change suggests that earthquake populations on a regional scale could also progressively evolve from Gutenberg–Richter to characteristic earthquake type behaviour (Wesnousky, 1994; Cowan et al., 1996). As with most studies of ancient faults in the subsurface, we assume that fault growth is driven by earthquake movements; whether or not the faults of this study area were aseismic does not, however, affect our conclusions regarding the progressive strain localisation within fault systems.

2. Fault geometry

The growth of normal fault systems within extensional basins can be analysed in detail where the faults intersected

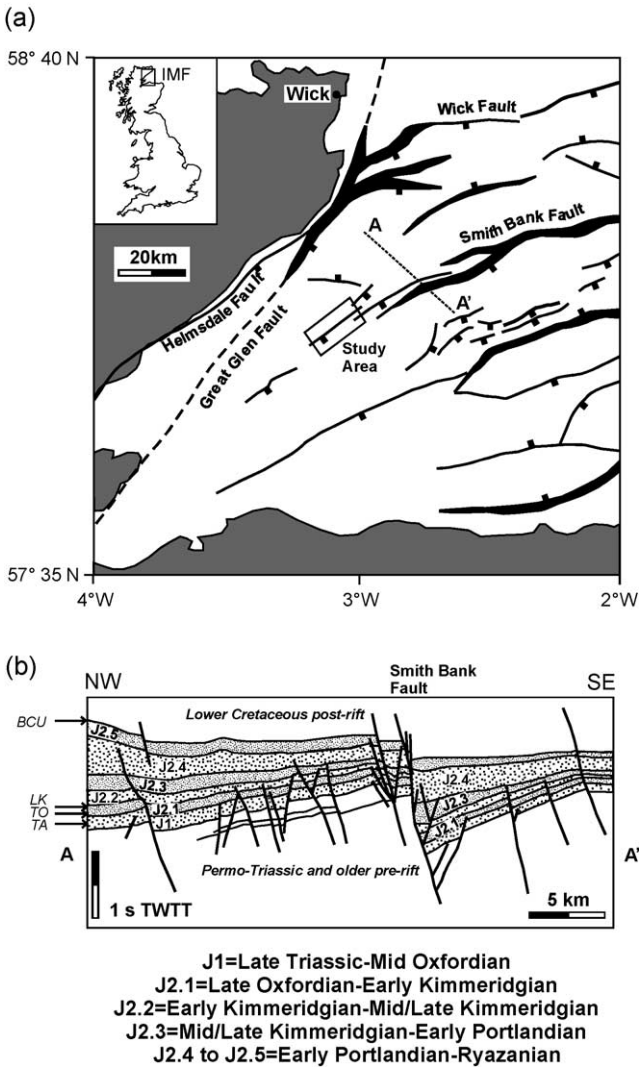

Fig. 2. (a) Map showing the principal Mesozoic structures in the Inner Moray Firth (IMF). Faults shown with solid lines accommodated mainly dip-slip displacements (black squares on the down-thrown side), whilst the sub-vertical Great Glen Fault (dashed line) originated as a strike-slip fault. The box shows the location of the 15 km × 6.5 km 3-D seismic survey, the finely dashed line (A–A′) shows the regional cross-section in (b). (b) Line drawing of a 2-D seismic reflection line showing the main structural elements and stratigraphic sub-divisions in the Inner Moray Firth (after Underhill, 1991a). The Late Jurassic syn-faulting sediments (stippled) thicken into the hanging walls, and thin onto the footwalls of major normal faults (e.g. Smith Bank Fault). The named horizons (TA = Top A; TO = Top Oxfordian; LK = Lower Kimmeridgian; BCU = Base Cretaceous Unconformity) correspond to horizons mapped throughout the 3-D seismic survey volume (Fig. 3).

the earth's surface and their displacement history is recorded by thickness and displacement changes within syn-faulting sediments (Childs et al., 1993, 1995). This is possible only where sedimentation rates exceed fault displacement rates (Nicol et al., 1997), a condition which is not satisfied by the many extensional basins characterised by relatively rapid fault displacement rates, with the formation of fault scarps, the erosion of uplifted footwalls and the underfilling of hanging wall basins (Contreras et al.,

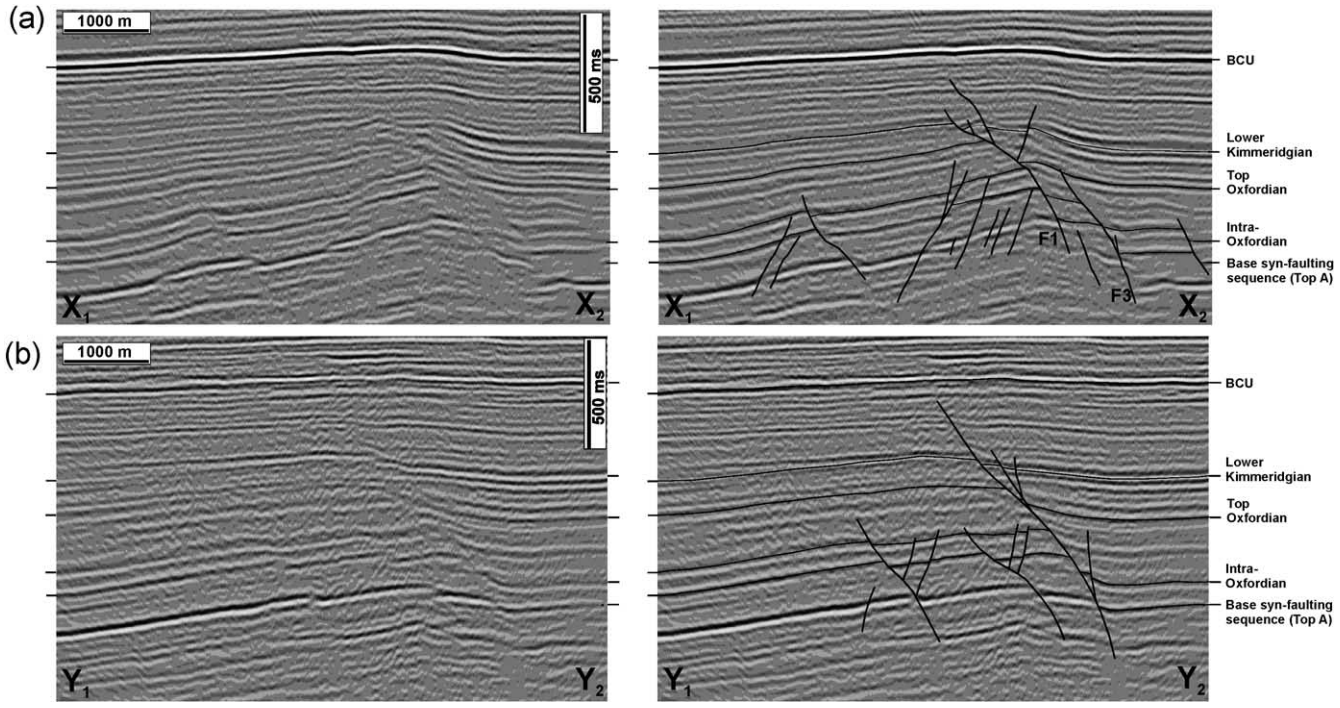

Fig. 3. Seismic sections oriented perpendicular to fault strike across the 15 km × 6.5 km study area. Seismic line spacing is 100 m, and the locations of the sections are shown in Fig. 4. The Top A horizon is of Late Callovian age and defines the base of the syn-faulting sedimentary sequence; the Intra-Oxfordian, Top Oxfordian and Lower Kimmeridgian horizons occur within the syn-faulting sequence. BCU is the Base Cretaceous Unconformity. (a) Uninterpreted and interpreted sections through a breached relay zone in the central part of the study area. F1 is the footwall fault, F3 is part of the hanging wall fault (see Fig. 4a). (b) Uninterpreted and interpreted sections through the southwestern part of the study area, 5.7 km along strike from (a).

2000). The availability of high quality, ideally 3-D, seismic datasets providing several well defined and dated horizons is a further requirement for the kinematic analysis of fault systems. Since these conditions are rarely met by most datasets, conclusions derived from their analysis are suspect (e.g. Contreras et al., 2000). In this study, using constraints from 3-D seismic data, we define the growth of a normal fault system in the Inner Moray Firth, which satisfies the basic geological conditions for the kinematic analysis of faults.

Blanketing of fault scarps by sediments and the preservation of fault displacement histories is a feature of the Inner Moray Firth (Underhill, 1991a,b; Nicol et al., 1997), a subbasin of the Upper Jurassic North Sea Basin, which is otherwise characterised by relatively low sedimentation rates and the development of large, sometimes kilometre-scale, fault scarps. Synsedimentary faults in the Inner Moray Firth were active during a ca. 16 Ma phase of rifting (Underhill, 1991a,b; Nicol et al., 1997). Within the basin, footwall erosion is restricted to the larger displacement portions of kilometre-scale faults outside the study area (Underhill 1991a,b): this observation is consistent with the fact that larger displacement faults have higher displacement rates than smaller displacement faults (Nicol et al., 1997; see below). As with fault studies in most other rift basins, we cannot entirely rule out the possibility that the structure of this study area has been partly inherited from a pre-existing underlying fault system. Although there is no evidence to suggest that this is the case (seismic data provide few constraints on underlying structures), it is nevertheless possible that the kinematic history of this fault system was, to some extent, influenced by older underlying structures (e.g. Meyer et al., 2002); the principal conclusions of this article are, however, independent of the underlying structure. What is clear however is that post-Cretaceous reactivation, with offset of the Base Cretaceous reflector, has occurred on some of the larger displacement faults within the basin (e.g. Thomson and Underhill, 1993; Fig. 2b), though it is not a feature of this study area.

Previous work in this basin suggests that fault displacement rate correlates with fault size and that smaller faults have higher mortality rates than larger faults (Nicol et al., 1997), features that have implications for the evolution of fault and earthquake populations. The aims of the present study were to better define the growth of a fault system and, in particular, fault populations from the analysis of a high-quality 3-D seismic dataset for a 15 km × 6.5 km area in the Inner Moray Firth: the area contains the Beatrice Field and the interpreted horizons are tied to proprietary well data. Specifically, we wanted to establish whether and how fault populations changed through time, and what implications such changes have for the evolution of fault arrays and earthquake faulting.

The seismic survey comprises 150 lines spaced at 100 m. The effective limit of resolution of the seismic data (i.e. the maximum throw above which all faults are resolved) is

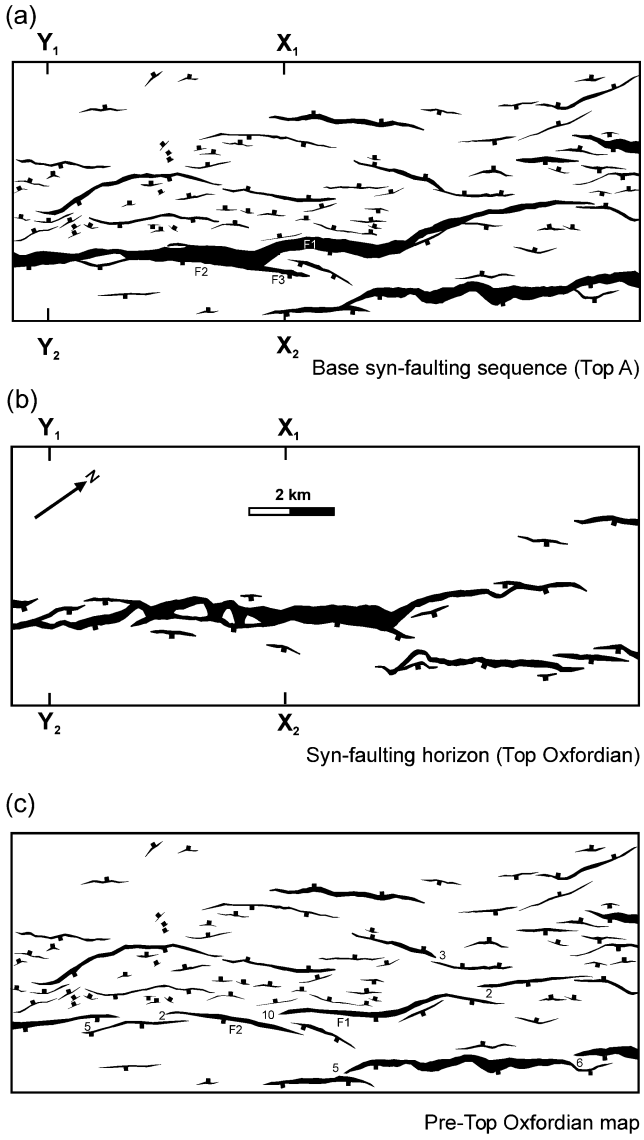

Fig. 4. Fault maps for (a) the base of the syn-faulting sequence (Top A), (b) within the syn-faulting sequence (Top Oxfordian) and (c) the Top A horizon backstripped to pre-Top Oxfordian times. The mapped reflectors are shown in Fig. 3. Heaves were determined by subtracting fault throws on the Top Oxfordian horizon from fault throws on the Top A horizon and then calculating the change in heave from the fault dip on each seismic line. Former fault segment boundaries are backstripped to their pre-linkage geometries and are each labelled with their approximate time of linkage in My after the onset of faulting. Fault dip direction is indicated by the filled squares. F1, F2 and F3 in (a) and (c) refer, respectively, to the footwall, hanging wall and inactive hanging wall splay faults associated with the breached relay zone discussed in the text.

estimated to be ca. 10 m but faults with maximum throws down to 5 m can be mapped. Errors associated with the mapping of fault tips are related to the lateral displacement gradients of faults and seismic line spacings (100 m) and are generally responsible for a decrease in the estimated fault length. For this dataset, the underestimation of fault length is no greater than ca. 150 m, an error which is acceptable for mapping purposes and for population analysis.

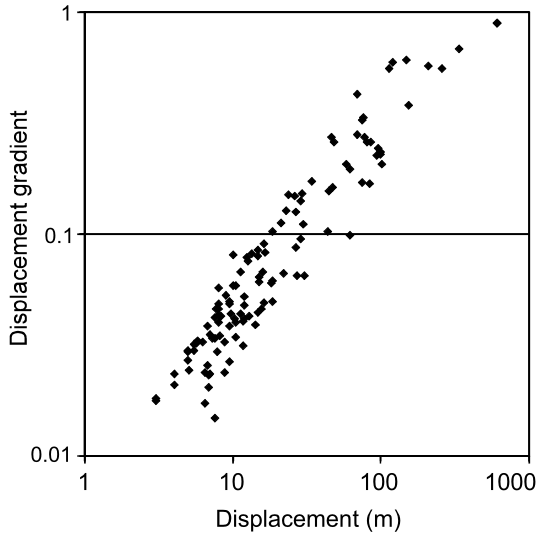

Fig. 5. Graph showing upward displacement gradient versus displacement for all faults in the study area that cut the Intra Oxfordian and/or Top A horizons; all gradients are positive indicating an upward decrease in displacement. Each point represents the average displacement and displacement gradient calculated for up to five seismic lines straddling the point of maximum displacement of each fault. The average displacement values can be significantly lower than the effective limit of resolution of the seismic dataset (i.e. 10 m; see text for details); estimated errors on average displacements are ±2.5 m and on average displacement gradients are ±0.01. For faults that cut both the Top A and Intra Oxfordian horizons (Fig. 4), the upward displacement gradient is calculated as the difference in displacement on the Top A and Intra Oxfordian horizons, divided by the along-fault distance between the two horizons. For faults that tip out above the level of the Top A horizon but do not intersect the overlying Intra Oxfordian horizon, the displacement on the Top A horizon has been divided by the thickness of the Top A to Intra Oxfordian interval to provide a minimum estimate of the upward displacement gradient.

The study area straddles the footwall high to a large normal fault (400 m maximum throw) that contains an array of normal faults. Towards the eastern boundary of the study area, displacement on the main fault is transferred, via fault relay zones, onto two other faults that downthrow in the same direction. There are approximately equal numbers of smaller faults that downthrow with, and in opposition to, the main faults (Figs. 3 and 4). The majority of faults show marked upward decreases in displacement, reflecting their synsedimentary nature, with less of the displacement history, and hence lower displacements, recorded on younger horizons.

Demonstration of a synsedimentary origin for upward displacement decreases permits kinematic analysis of a fault system as described in a later section. Large across-fault thickness changes and high displacement gradients associated with the large faults in the study area are clearly of synsedimentary origin. However the lower thickness changes and displacement gradients associated with the smaller faults overlap those associated with the fault propagation strains of blind, post-depositional faults. Quantitative analysis of the upward decreases in displacement, expressed as positive displacement gradients in Fig. 5, suggests,

however, that the smaller faults in the study area are also of synsedimentary origin. Displacement gradients have been computed for each fault on cross-sections straddling their point of maximum displacement. Displacement gradients are measured as the difference in displacement between an underlying and overlying horizon, divided by the distance between the mid-points of the cutoffs for each horizon. For faults that do not extend upwards into an overlying interpreted horizon, we have computed a minimum displacement gradient by assuming that the fault extends up to the overlying horizon. Data for all of the faults in the study area are shown on a plot of displacement gradient vs. displacement (Fig. 5). Faults with displacements in excess of ca. 30 m have upward displacement gradients which are greater than ca. 0.1, high values which are similar to those observed on synsedimentary faults from other areas (Nicol et al., 1996, 1997; Cartwright et al., 1998). For lower displacement faults, displacement gradients are lower and overlap with the higher end of values previously attributed to the propagation-related strains observed on post-depositional faults (<0.07; Nicol et al., 1996). This overlap for small displacement faults is inevitable given the resolution limits typical of seismic datasets and the broad range of displacement gradients seen on synsedimentary faults (displacement gradients of <0.07 have been recorded on synsedimentary faults; Nicol et al., 1996; Cartwright et al., 1998). There are, however, good grounds for suggesting that all faults, and not only those with displacements greater than ca. 30 m, are synsedimentary in origin. Previous studies have shown that normal faults within the Inner Moray Firth are synsedimentary, with upward decreases in displacement accompanied by sympathetic sequence thickening across faults (Underhill, 1991a,b; Nicol et al., 1997). A broad correlation between upward displacement changes (i.e. displacement gradients) and displacement (Fig. 5), is consistent with the growth behaviour previously observed in the Inner Moray Firth and in other fault systems, in which larger displacement faults move faster, with correspondingly higher upward displacement gradients, and are longer lived than smaller displacement faults (Nicol et al., 1997; Walsh et al., 2001; Meyer et al., 2002). Taken together, these lines of evidence favour a synsedimentary origin for all faults.

3. Fault growth

Examination of seismic sections across the study area shows that there is a clear positive relationship between vertical persistence, and therefore longevity of growth, and fault displacement (Fig. 3). Since larger displacement faults also have larger fault trace lengths, fault maps show that early phases of faulting and older horizons are characterised by many smaller faults, whilst later stages of faulting and younger syn-faulting horizons are faulted mainly by larger faults (Figs. 3 and 4). This evolution of structure and fault populations can be reconstructed using displacement backstripping methods in which displacements on younger horizons are subtracted from those of underlying horizons (Petersen et al., 1992; Childs et al., 1993).

Displacement backstripping is performed on individual cross-sections and is underpinned by the assumption that the displacement of a horizon records the post-depositional displacement on the fault. The difference in displacement between successive horizons is therefore a measure of the displacement accrued during the time interval between their deposition. Conversely, if the displacement on two horizons is the same then the fault must have intersected the cross-section after the deposition of the younger horizon. Furthermore, if a fault does not offset the overlying horizon then it must have died prior to deposition of that horizon. These three conditions permit backstripping to reconstruct fault system geometry at earlier stages of rifting (Fig. 4c).

For those faults which do not intersect the Top Oxfordian horizon, i.e. the large majority of faults, the error in backstripped fault lengths is the same as that associated with fault mapping (<ca 150 m). The restored lengths of fault segments which have linked to produce a single fault (see below) may be overestimated by up to 300 m. These restored segments have lengths greater than 2 km so that a possible 15% overestimate of length does not impact the population analysis described below. In the study area the difference in compaction over the ca. 350 m shale dominated interval between the Top A and Top Oxfordian horizons, for a standard porosity depth function, results in a ca. 3% underestimate of the backstripped throws; the effects of compaction can therefore be ignored.

The principal characteristic of the studied fault system at early stages is that it comprises a broad size range of poorly connected faults (Fig. 4c). By contrast, the fault system at later stages of faulting is dominated by larger faults that extend almost across the entire study area (Fig. 4b). Apart from relay breaching and associated linkage, lateral propagation of faults is not observed in the thickness variations within the synsedimentary sequence, i.e. variation in the timing of movement on individual faults along their length is not recorded, even for the largest faults in the area. Our analysis suggests, therefore, that the basic fault pattern was established prior to deposition of the youngest mappable syn-rift horizon and using the biostratigraphic constraints of Underhill (1991a,b), within ~3 My of the beginning of the 16-My-period of rifting. Therefore, propagation mainly occurred early in the growth of the fault system, a feature that is consistent with a recently developed growth model for faults (Walsh et al., 2002). Later evolution of the fault system, the subject of this paper, is dominated by fault linkage and relay zone breaching.

An example of fault linkage, between faults F1 and F2, is illustrated on the cross-section in Fig. 3a and the present day and restored maps in Fig. 4a and c, respectively. The cross-section is through the western end of fault F1 where the throws on this fault are similar on both the Top A and the

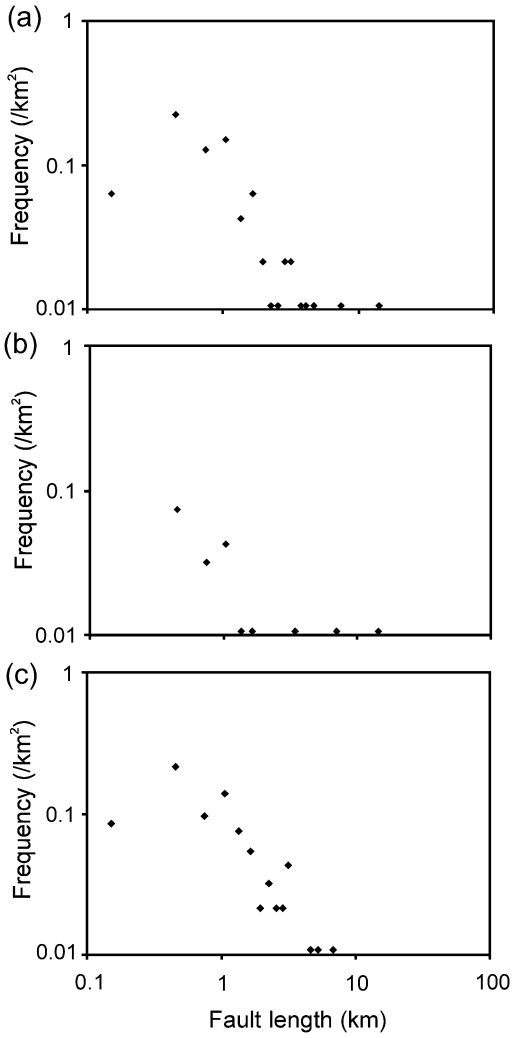

Fig. 6. Fault length populations expressed in terms of frequency/area for (a) the pre-faulting Top A horizon (b) the syn-faulting Top Oxfordian horizon and (c) the pre-Top Oxfordian map. The interpreted horizons and associated fault maps are shown in Figs. 3 and 4.

Top Oxfordian horizons. To the east of the cross-section Top A throws are significantly greater than those on the Top Oxfordian, while 200 m to the west and close to the branchpoint between F1 and F2, the throws are identical. These throw variations demonstrate that the western portion of F1 was not present at Top Oxfordian times (Fig. 4c) and that linkage of faults F1 and F2 occurred following deposition of the Top Oxfordian horizon. Linkage resulted in the death of the portion of F2 in the hanging wall of the new continuous fault, labelled F3 in Fig. 4a. F3 extends to a position just above the Top Oxfordian (Fig. 3a) indicating that the death of F3 was approximately synchronous with the linkage of F1 and F2.

Linkage between F1 and F2 occurred approximately at the time of deposition of the Top Oxfordian horizon, ca. 10 My after the initiation of faulting. Each of the mapped former segment boundaries has been backstripped to the time of linkage using the approach described above (Fig. 4c). Many of the breaching events occurred between the times of deposition of the mapped horizons, and approximate timing of each breaching event is obtained from the elevation of the upper tip of the dead splay by assuming a constant sedimentation rate in the interval between overlying and underlying mapped horizons. The variable timing of breaching of the segment boundaries demonstrates a progressive linkage of the fault system through time.

4. Fault populations

Quantitative aspects of the evolution of the fault system can be highlighted from fault population studies. Fault populations for different stages of growth of the system are plotted on logarithmic plots of fault size vs. frequency (Fig. 6), a method that is more sensitive to variations in population parameters than the more usual cumulative frequency curves used in many population studies (see Pickering et al., 1995 for details). The sizes of faults are presented in terms of their trace length on fault maps. The slopes of population curves measured from this 2-D sampling scheme can be related to those of other, i.e. 1-D and 3-D, sampling domains and of different measures of fault size, such as displacement (in 1-D), maximum displacement or geometric moment (Marrett and Allmendinger, 1991; Walsh et al., 1991; Westaway, 1994). Population curves for the present day fault system recorded on pre-faulting horizons describe a power-law distribution (with slope of ca. −1.7) for fault trace lengths ranging from ca. 4 km down to ca. 300 m (Fig. 6a). The lower limit of fault trace length is controlled mainly by the lengths of faults with maximum displacements that can be resolved seismically (ca. 10 m). The upper limit does not however correspond to the largest faults, two of which have lengths (7and 14 km) that are in excess of the maximum expected from the power-law population. Fault populations on younger syn-faulting horizons show similar characteristics, but with a more weakly developed power-law distribution defined at even lower fault sizes (ca. 1 km to 300 m; Fig. 6b). Fault populations for different aged horizons therefore contain the same larger faults, but are distinguished mainly by a decrease in the numbers of smaller faults on younger horizons. This difference reflects the fact that although some small faults were active throughout the growth of the fault system, smaller faults generally have higher mortality rates than larger faults and few smaller faults initiate later in the evolution of the system.

The present-day fault system has power-law length distributions with the largest faults in the system occupying clear non-power-law tails on both pre-rift and syn-rift horizons. The contrast with the fault size distributions during rifting is highlighted by the backstripped fault population that defines a power-law distribution over the entire range of fault size (with a slope of ca. −1.4; Fig. 6c). At this stage of evolution of the fault system (Fig. 4c) the larger and longer faults had

yet to form fully and the system was less well connected than it is at present (Fig. 4b). With continued growth of the fault system, medium sized faults linked to provide larger faults that extend almost across the entire map area. At this stage most of the smaller faults died and continued displacements were thereafter concentrated on the larger faults. This concentration resulted in the development of the non-power-law tail observed on the present-day pre-rift horizon (Fig. 6b).

5. Discussion

The evolution of structure in the study area is characterised principally by progressive strain localisation onto larger faults, a process that appears to be controlled by the connectivity of faults at the scale of the mapped area. This model is consistent with previous work on the Inner Moray Forth presented by Nicol et al. (1997), suggesting that larger faults are longer lived than smaller faults. The model is also consistent with conceptual models for the breaching of relays and the linkage of associated fault segments (Peacock and Sanderson, 1991; Ramsay and Huber, 1987; Cartwright et al., 1995; Childs et al., 1995). Geometrically similar localisation phenomena have been described on a much smaller scale from laboratory experiments, in which process zones characterised by discontinuous networks of small cracks precede the formation of a through-going fracture (Main et al., 1990a,b; Main, 1992). Such systems are also characterised by a change in the populations of fractures from power-law to non-power law. Recent analogue modelling studies have also shown that progressive strain localisation is an important characteristic of the growth of fault systems (Ackermann et al., 2001; Mansfield and Cartwright, 2001), even showing population changes which are reminiscent of this natural fault system (Ackermann et al., 2001). Numerical and geometric models of faulting also suggest that, with continued displacement, populations of faults evolve into longer and simpler systems (Sornette et al., 1990; Cowie et al., 1995; Cowie, 1998; Gupta et al., 1998). Strain localisation onto through-going faults may therefore be a fundamental characteristic of the spatial and temporal evolution of fault systems, occurring at progressively larger scales over progressively longer periods. Once a through-going fault is developed at a given scale, the system is scale-bound at that scale and will develop non-power law active fault populations. There is a causal link between through-going, i.e. connected, fault systems and strain localisation, because such systems represent the most efficient means of accommodating fault-related deformation.

We expect that the strain localisation we observe in the Inner Moray Firth on a 15 km scale, is likely to have been preceded by geometrically similar processes occurring on smaller, e.g. 1 km, scales throughout the evolution of the fault system. The localisation phenomenon is, however, only identifiable from our dataset at the large scale range owing to the resolution of the seismic data. We would also expect the same localisation process to have operated on a more regional scale, i.e. basin scale, with displacement progressively concentrated onto larger faults some of which are longer lived than the largest fault in the study area: future work may permit this hypothesis to be tested.

The consequences of strain localisation for the evolution of fault populations are that the active population of faults will become scale-bound at increasingly larger scales, with through-going faults continuing to grow at the expense of smaller, less well connected, faults. The scaling properties of the active fault population will therefore progressively change from power-law through to non-power-law. The most significant aspect of the localisation process is, however, that the relative numbers of active small faults and the strain they accommodate, decreases relative to that of the larger faults. A similar decrease in the contribution of small faults, with a gradual shallowing of the active fault population slope, has been established from studies in the Timor Sea (Meyer et al., 2002). In that case, the absence of non-power law tails for seismically-resolvable faults has been attributed to the less evolved nature of the fault system in which one or more through-going faults are not developed at the scale of observation (Meyer et al., 2002). Although both systems are characterised by rapid development of the basic fault pattern, a feature that is consistent with a new model for fault growth (Walsh et al., 2002), the Inner Moray Firth fault system highlights the importance of subsequent fault linkage across relays and the associated death of most of the small faults.

The question arises as to how and whether strain localisation phenomena can be identified from other datasets. A prerequisite for directly identifying such changes is kinematic control on fault system development. For most datasets, however, the kinematics of faulting cannot be established unequivocally, because sedimentation rates usually do not exceed the displacement rates of a population of faults and the fault displacement history is therefore rarely preserved. Indirect evidence for strain localisation is provided by the presence of non-power-law tails at large fault sizes. These tails are not, however, easily identifiable from the more often used cumulative frequency plots. For example, the populations of pre-rift horizons of this study area show only a slight irregularity at larger fault sizes with a shallowing of the entire population slope. A progressive shallowing of cumulative frequency population slopes towards smaller fault sizes is one characteristic that would be predicted from this strain localisation model. Observational support for this type of behaviour has been advanced from the study of fault populations over very large scale ranges (several orders of magnitude of fault size; Nicol et al., 1996). In the absence of kinematic data, however, it will always be difficult, if not impossible, to distinguish populations that reflect the temporal evolution of the system from those that are due to the expected variations in populations arising from the spatial characteristics, i.e. clustering, of the fault system.

Progressive strain localisation onto larger faults during fault system evolution must be reconciled with evidence from earthquake studies. Any change in the character of the active population of a fault system demands some changes in the earthquake populations. Relating the active fault population to earthquake populations is not straightforward. It has long been established that for active faults, the average coseismic displacement scales with earthquake rupture length (Scholz, 1982; Scholz et al., 1986). Since individual faults do not always rupture over their entire surface and some earthquake ruptures operate on a number of adjacent segments, a direct equivalence between earthquake rupture length and fault length does not apply. A broad equivalence is supported, however, by the concept of the characteristic earthquake model, and related supporting data (Wesnousky et al., 1983; Wesnousky, 1994, 1999), and is one of the basic tenets of existing growth models for faults (Walsh and Watterson, 1987; Cowie and Scholz, 1992a,b,c; Gillespie et al., 1992). The characteristic earthquake model also suggests that although large earthquakes occur on large faults, the largest earthquakes on an individual fault are also accompanied by a power-law population of smaller earthquakes, with a significant gap between the largest earthquakes and the small earthquake population (Wesnousky, 1994). The scaling properties of the characteristic earthquake model are therefore very similar to those of the later stages of growth of our natural fault system. Since the scaling properties of fault populations during the early stages of growth of this fault system are power-law and therefore reminiscent of the Gutenberg–Richter earthquake scaling law, differences in the scaling properties of earthquakes may, by analogy with fault populations, partly reflect the spatio-temporal evolution of fault systems. This type of behaviour is very similar to models advanced to explain both earthquake observations (Robertson et al., 1995; Wesnousky, 1999) and the results of numerical models of fault system growth (Cowie, 1998). Earthquake populations within tectonically active terrains may therefore show scaling properties that evolve from Gutenberg–Richter through to characteristic earthquake behaviour with increasing maturity of the system, a feature that has direct implications for earthquake hazard assessment.

6. Conclusions

1. Active fault size populations of a normal fault system in the Inner Moray Firth basin evolved from power-law to non-power-law.
2. The basic fault pattern was established early, prior to deposition of the youngest mappable syn-rift horizon and within the first 3 My of the 16-My-rifting period.
3. Faulting became increasingly localised onto the largest faults, with smaller faults preferentially dying and making a diminishing contribution to fault-related strain.
4. Smaller, dead, faults contribute a stable power-law shadow to an increasingly scale-bound system.
5. Strain localisation onto fewer and better connected faults represents a progression towards the most efficient means of accommodating fault-related deformation, and is considered to be a fundamental characteristic of the spatio-temporal evolution of fault systems.
6. Progressive strain localisation during fault system evolution requires complementary changes in earthquake populations and favours a model in which Gutenberg–Richter, i.e. power-law, earthquake populations give way to characteristic earthquake, i.e. non-power-law, earthquake populations as the fault system matures.

Acknowledgements

We are grateful to former staff at Britoil and BP for provision of the seismic data. Thanks to Patience Cowie and Joe Cartwright for their useful reviews of the manuscript and to members of the Fault Analysis Group for helpful discussion. The work was partly funded by an Enterprise Ireland Basic Research Grant (Contract No. SC/2001/141).

References

Ackermann, R.V., Schlische, R.W., Withjack, M.O., 2001. The geometric and statistical evolution of normal fault systems: an experimental study of the effects of mechanical layer thickness on scaling laws. Journal of Structural Geology 23, 1803–1819.

Cartwright, J.A., Trudgill, B., Mansfield, C., 1995. Fault growth by segment linkage: an explanation for scatter in maximum displacement and trace length data from Canyonlands Grabens of SE Utah. Journal of Structural Geology 17, 1319–1326.

Cartwright, J., Bouroullec, R., James, D., Johnson, H., 1998. Polycyclic motion history of some Gulf Coast growth faults from high-resolution displacement analysis. Geology 26, 819–822.

Childs, C., Walsh, J.J., Watterson, J., 1990. A method for estimation of the density of fault displacements below the limits of seismic resolution in reservoir formations. In: Buller, A.T., Berg, E., Hjelmeland, O., Kleppe, J., Torsæter, O., Aasen, J.O. (Eds.). North Sea Oil and Gas Reservoirs II. Graham & Trotman, London, pp. 309–318.

Childs, C., Easton, S.J., Vendeville, B.C., Jackson, M.P.A., Lin, S.T., Walsh, J.J., Watterson, J., 1993. Kinematic analysis of faults in a physical model of growth faulting above a viscous salt analogue. Tectonophysics 228, 313–329.

Childs, C., Watterson, J., Walsh, J.J., 1995. Fault overlap zones within developing normal fault systems. Journal of the Geological Society 152, 535–549.

Contreras, J., Anders, M.H., Scholz, C.H., 2000. Growth of a normal fault system: observations from the Lake Malawi basin of the east African rift. Journal of Structural Geology 22, 159–168.

Cowan, H., Nicol, A., Tonkin, P., 1996. A comparison of historical and paleoseismicity in a newly formed fault zone and a mature fault zone, North Canterbury, New Zealand. Journal of Geophysical Research—Solid Earth 101, 6021–6036.

Cowie, P.A., 1998. A healing-reloading feedback control on the growth rate of seismogenic faults. Journal of Structural Geology 20, 1075–1087.

Cowie, P.A., Scholz, C.H., 1992a. Displacement–length scaling relationship for faults: data synthesis and discussion. Journal of Structural Geology 14, 1149–1156.

Cowie, P.A., Scholz, C.H., 1992b. Growth of faults by accumulation of

seismic slip. Journal of Geophysical Research—Solid Earth 97, 11085–11095.

Cowie, P.A., Scholz, C.H., 1992c. Physical explanation for displacement–length relationship for faults using a post-yield fracture mechanics model. Journal of Structural Geology 14, 1133–1148.

Cowie, P.A., Sornette, D.C., Vanneste, C., 1995. Multifractal scaling properties of a growing fault population. Geophysical Journal International 122, 457–469.

Gillespie, P.A., Walsh, J.J., Watterson, J., 1992. Limitations of dimension and displacement data from single faults and the consequences for data analysis and interpretation. Journal of Structural Geology 14, 1157–1172.

Gupta, S., Cowie, P.A., Dawers, N.H., Underhill, J.R., 1998. Mechanism to explain rift basin subsidence and stratigraphic patterns through fault array evolution. Geology 26, 595–598.

Kakimi, T., 1980. Magnitude-frequency relation for displacement of minor faults and its significance in crustal deformation. Bulletin of the Geological Survey of Japan 31, 467–487.

Main, I.G., 1992. Damage mechanics with long-range interactions: correlation between the seismic b-value and the fractal two-point correlation dimension. Geophysical Journal International 111, 531–541.

Main, I.G., Meredith, P.G., Sammonds, P.R., Jones, C., 1990. Influence of fractal flaw distributions on rock deformation in the brittle field. In: Knipe, R.J., Rutter, E.H. (Eds.), Deformation Mechanisms, Rheology and Tectonics. Geological Society Special Publication 54, pp. 81–96.

Main, I.G., Peacock, P.G., Meredith, P.G., 1990b. Scattering attenuation and the fractal geometry of fracture systems. Pure and Applied Geophysics 133, 283–304.

Mansfield, C., Cartwright, J., 2001. Fault growth by linkage: observations and implications from analogue models. Journal of Structural Geology 23, 745–763.

Marrett, R., Allmendinger, R.W., 1991. Estimates of strain due to brittle faulting: sampling of fault populations. Journal of Structural Geology 13, 735–738.

Meyer, V., Nicol, A., Childs, C., Walsh, J.J., Watterson, J., 2002. Progressive localisation of strain during the evolution of a normal fault system in the Timor Sea. Journal of Structural Geology 24, 1215–1231.

Nicol, A., Walsh, J.J., Watterson, J., Gillespie, P.A., 1996. Fault size distributions—are they really power law? Journal of Structural Geology 18, 191–197.

Nicol, A., Walsh, J.J., Watterson, J., Underhill, J.R., 1997. Displacement rates of normal faults. Nature 390, 157–159.

Peacock, D.C.P., Sanderson, D.J., 1991. Displacements, segment linkage and relay ramps in normal fault zones. Journal of Structural Geology 13, 721–733.

Petersen, K., Clausen, O.R., Korstgård, J.A., 1992. Evolution of a salt-related listric growth fault near the D-1 well, block 5605, Danish North Sea: displacement history and salt kinematics. Journal of Structural Geology 14, 565–577.

Pickering, G., Bull, J.M., Sanderson, D.J., 1995. Sampling power-law distributions. Tectonophysics 248, 1–20.

Pickering, G., Bull, J.M., Sanderson, D.J., 1996. Scaling of fault displacements and implications for the estimation of sub-seismic strain. In: Buchanan, P.G., Nieuwland, D.A. (Eds.), Modern Developments in Structural Interpretation, Validation and Modelling. Geological Society Special Publication 99, pp. 11–26.

Ramsay, J.G., Huber, M.I., 1987. The Techniques of Modern Structural Geology. Volume 2: Folds and Fractures. Academic Press, London.

Robertson, M.C., Sammis, C.G., Sahimi, M., Martin, A.J., 1995. Fractal analysis of three dimensional spatial distributions of earthquakes with a percolation interpretation. Journal of Geophysical Research—Solid Earth 100, 609–620.

Scholz, C.H., 1982. Scaling laws for large earthquakes: consequences for physical models. Bulletin of the Seismological Society of America 72, 1–14.

Scholz, C.H., 1989. Mechanics of faulting. American Review of Earth and Planetary Sciences 17, 304–334.

Scholz, C.H., Cowie, P.A., 1990. Determination of total strain from faulting using slip measurements. Nature 346, 837–839.

Scholz, C.H., Aviles, C.A., Wesnousky, S.G., 1986. Scaling differences between large interplate and intraplate earthquakes. Bulletin of the Seismological Society of America 76, 65–70.

Schwartz, D.P., Coppersmith, K.J., 1984. Fault behavior and characteristic earthquakes: examples from the Wasatch and San Andreas Fault Zones. Journal of Geophysical Research—Solid Earth 89, 5681–5698.

Sornette, D., Davy, P., Sornette, A., 1990. Structuration of the lithosphere in plate tectonics as a self-organized critical phenomenon. Journal of Geophysical Research—Solid Earth 95, 17353–17361.

Thomson, K., Underhill, J.R., 1993. Controls on the development and evolution of structural styles in the Inner Moray Firth Basin. In: Parker, J.R. (Ed.). Petroleum Geology of Northwest Europe: Proceedings of the 4th Conference. , pp. 1167–1178.

Underhill, J.R., 1991a. Controls on Late Jurassic seismic sequences, Inner Moray Firth, UK North Sea: a critical test of a key segment of Exxon's original global cycle chart. Basin Research 3, 79–98.

Underhill, J.R., 1991b. Implications of Mesozoic–Recent basin development in the western Inner Moray Firth, UK. Marine and Petroleum Geology 8, 359–369.

Walsh, J.J., Watterson, J., 1987. Distributions of cumulative displacement and seismic slip on a single normal fault surface. Journal of Structural Geology 9, 1039–1046.

Walsh, J.J., Watterson, J., 1988. Analysis of the relationship between the displacements and dimensions of faults. Journal of Structural Geology 10, 239–247.

Walsh, J.J., Watterson, J., Yielding, G., 1991. The importance of small-scale faulting in regional extension. Nature 351, 391–393.

Walsh, J.J., Watterson, J., Yielding, G., 1994. Determination and interpretation of fault size populations: procedures and problems. In: Aasen, J.O., Berg, E., Buller, A.T., Hjelmeland, O., Holt, R.M., Kleppe, J., Torsæter, O. (Eds.). North Sea Oil and Gas Reservoirs III. Kluwer Academic Publishers, London, pp. 141–155.

Walsh, J.J., Childs, C., Meyer, V., Manzocchi, T., Imber, J., Nicol, A., Tuckwell, G., Bailey, W.R., Bonson, C.G., Watterson, J., Nell, P.A.R., Strand, J.A., 2001. Geometrical controls on the evolution of normal fault systems. In: Holdsworth, R.E., Strachan, R.A., Magloughlin, J.F., Knipe, R.J. (Eds.), The Nature and Tectonic Significance of Fault Zone Weakening. Geological Society Special Publication 186, pp. 157–170.

Walsh, J.J., Nicol, A., Childs, C., 2002. An alternative model for the growth of faults. Journal of Structural Geology in press.

Wesnousky, S.G., 1994. The Gutenberg–Richter distribution or characteristic earthquake distribution: which is it? Bulletin of the Seismological Society of America 84, 1940–1959.

Wesnousky, S.G., 1999. Crustal deformation processes and the stability of the Gutenberg–Richter relationship. Bulletin of the Seismological Society of America 89, 1131–1137.

Wesnousky, S.G., Scholz, C.H., Shimazaki, K., Matsuda, T., 1983. Earthquake frequency distribution and the mechanics of faulting. Journal of Geophysical Research—Solid Earth 88, 9331–9340.

Westaway, R., 1994. Quantitative analysis of populations of small faults. Journal of Structural Geology 16, 1259–1273.

Yielding, G., Needham, T., Jones, H., 1996. Sampling of fault populations using sub-seismic data: a review. Journal of Structural Geology 18, 135–146.